Automatica 146 (2022) 110579

Contents lists available at ScienceDirect

Automatica

journal homepage: www.elsevier.com/locate/automatica

Brief paper

Online optimization of switched LTI systems using continuous-time and hybrid accelerated gradient flows☆

Gianluca Bianchin [a,*], Jorge I. Poveda [c], Emiliano Dall'Anese [b]

[a] Institute of Information and Communication Technologies, Electronics and Applied Mathematics, University of Louvain, Louvain-la-Neuve, 1348, Belgium
[b] Department of Electrical, Computer, and Energy Engineering, University of Colorado, Boulder, CO, 80309, USA
[c] Department of Electrical and Computer Engineering, University of California, San Diego, CA, 92093, USA

ARTICLE INFO

Article history:
Received 11 August 2020
Received in revised form 18 February 2022
Accepted 15 July 2022
Available online 15 September 2022

ABSTRACT

This paper studies the design of feedback controllers to steer a switching linear dynamical system to the solution trajectory of a time-varying convex optimization problem. We propose two types of controllers: (i) a continuous controller inspired by the online gradient descent method, and (ii) a hybrid controller that can be interpreted as an online version of Nesterov's accelerated gradient method with restarts of the state variables. By design, the controllers continuously steer the system toward a time-varying optimal equilibrium point without requiring knowledge of exogenous disturbances affecting the system. For cost functions that are smooth and satisfy the Polyak–Łojasiewicz inequality, we demonstrate that the online gradient-flow controller ensures uniform global exponential stability when the time scales of the system and controller are sufficiently separated and the switching signal of the system varies slowly on average. For cost functions that are strongly convex, we show that the hybrid accelerated controller can outperform the continuous gradient descent method. When the cost function is not strongly convex, we show that the hybrid accelerated method guarantees global practical asymptotic stability.

1. Introduction

In this paper, we investigate the use of online optimization algorithms for the control of switching dynamical systems. We consider linear time-invariant (LTI) plants with state $x \in \mathbb{R}^n$, output $y \in \mathbb{R}^p$, and dynamics

$$\begin{aligned} \dot{x} &= A_\sigma x + B_\sigma u + E_\sigma \omega_t := P_\sigma(x, u, \omega_t), \\ y &= Cx + D\omega_t \qquad\quad := h(x, \omega_t), \end{aligned} \tag{1}$$

where $\omega_t : \mathbb{R}_{\geq 0} \to \mathbb{R}^q$ is an unknown exogenous disturbance (here, the subscript t emphasizes time dependence), $u \in \mathbb{R}^m$ is the control input, $\sigma : \mathbb{R}_{\geq 0} \to \mathcal{S}$ is a piece-wise continuous switching signal taking values in the finite set $\mathcal{S} := \{1, 2, \dots, S\}$, with $S \in \mathbb{N}$, and $A_\sigma, B_\sigma, E_\sigma, C, D$ are matrices of appropriate dimensions. The goal is to steer the inputs and outputs of (1) towards the time-varying solutions of the problem:

$$\begin{aligned} &\min_{u,x,y} \ \ \phi_u(u) + \phi_y(y), \\ &\text{s.t.} \ \ P_\sigma(x, u, \omega_t) = 0, \quad y = h(x, \omega_t), \end{aligned} \tag{2}$$

where $\phi_u : \mathbb{R}^m \to \mathbb{R}$ and $\phi_y : \mathbb{R}^p \to \mathbb{R}$ embed performance metrics associated with the steady-state inputs and outputs of the system, respectively. Notice that, because (2) is parametrized by the time-varying signal ω_t, its solutions are time-varying and thus define *optimal trajectories*. The control objective (2) can be interpreted as an equilibrium-selection problem, where the goal is to select at every time the equilibrium points of (1) that minimize the cost in (2). This class of optimization problems has emerged in several engineering applications (Bianchin, Cortés, Poveda, & Dall'Anese, 2021; Brunner, Dürr, & Ebenbauer, 2012; Colombino, Dall'Anese, & Bernstein, 2020; Hauswirth, Bolognani, Hug, & Dörfler, 2020; Jokic, Lazar, & Bosch, 2009; Lawrence, Nelson, Mallada, & Simpson-Porco, 2018; Lawrence, Simpson-Porco, & Mallada, 2020; Menta, Hauswirth, Bolognani, Hug, & Dörfler, 2018; Zheng, Simpson-Porco, & Mallada, 2020), including power systems (Colombino et al., 2020; Menta et al., 2018) and transportation systems (Bianchin et al., 2021; Bianchin & Pasqualetti, 2020), where the time-variability of ω_t precludes the use of off-line solutions to (2) for the purpose of real-time control.

☆ The material in this paper was not presented at any conference. This paper was recommended for publication in revised form by Associate Editor Daniele Casagrande under the direction of Editor Ian R. Petersen.

* Corresponding author.
E-mail addresses: gianluca.bianchin@colorado.edu (G. Bianchin), poveda@ucsd.edu (J.I. Poveda), emiliano.dallanese@coloradoe.edu (E. Dall'Anese).

https://doi.org/10.1016/j.automatica.2022.110579
0005-1098/

Optimization-based controllers for (1)–(2) were studied in Menta et al. (2018) when ω_t is constant and the plant does not switch. The authors considered low-gain gradient-flow controllers of the form:

$$\dot{u} = -\eta \nabla \Phi(u, y), \tag{3}$$

where Φ is a modified cost function and $\eta > 0$ is a small tunable gain. This approach was extended to smooth nonlinear plants and controllers in Hauswirth et al. (2020) using singular perturbation tools (Khalil, 2002, Ch. 11). Joint stabilization and regulation problems related to (2) were the focus of Lawrence et al. (2020) and Lawrence et al. (2018) for a class of smooth systems. For LTI systems under time-varying disturbances, problem (2) was addressed in Colombino et al. (2020) via integral quadratic constraints, providing conditions that guarantee exponential stability and bounded tracking errors. Similar time-varying settings for feedback-linearizable plants were considered in Zheng et al. (2020). Controllers based on saddle-point flows where considered in Bianchin et al. (2021) for problems with linear inequality constraints on y.

Despite the above line of work, optimization-based controllers for systems with switching dynamics have not been studied yet. These systems are prevalent in engineering applications where plants are characterized by multiple operating modes; these include transportation networks, where multiple modes originate, e.g., due to the switching nature of traffic lights, and power grids, whose dynamics have often several operating modes due to switching hardware. For these systems, it remains an open question whether optimization-based controllers can still be applied, and under what conditions on the switching signal it is possible to guarantee their convergence. In this work, we provide an answer to these questions by presenting new stability results for optimization-based controllers applied to switched LTI systems. By using Lyapunov-based tools for set-valued hybrid dynamical systems (HDS) (Goebel, Sanfelice, & Teel, 2012) and the notion of input-to-state stability (ISS), we show that an average dwell-time constraint (Hespanha & Morse, 1999) is sufficient to guarantee closed-loop stability, provided that the time scales of the plant and the controller are suitably separated.

One of the well-known disadvantages of gradient-flow methods in the convex optimization literature is that their rate of convergence is bounded by the fundamental limit $\mathcal{O}(1/t)$ (Wibisono, Wilson, & Jordan, 2016). Naturally, this limitation extends to cases where gradient flows are utilized for controlling dynamical systems under time scale separation, as in (3). A natural question to ask is whether *accelerated* methods, such as those studied in Su, Boyd, and Candes (2014), can also be used as feedback controllers for dynamical systems. We address this question by studying controllers inspired by a family of ODEs with dynamic momentum of the form:

$$\ddot{u} + \frac{p+\dot{\tau}}{\tau}\dot{u} + p^2\tau^{p-2}k\nabla\Phi(u,y) = 0, \tag{4}$$

where τ denotes time, $p \geq 2$, and $k > 0$ is a gain. Systems of this form have recently received attention due to their ability to optimize smooth convex cost functions at a rate of $\mathcal{O}(1/\tau^p)$ (Su et al., 2014; Wibisono et al., 2016). While different versions of (4) have been explored for classical optimization problems (see Gaudio, Annaswamy, Bolender, and Lavretsky (2021), Poveda and Li (2021), Shi, Du, Jordan, and Su (2021) and Zhang, Uribe, Mokhtari, and Jadbabaie (2018)), the authors in Su et al. (2014) and Wibisono et al. (2016) showed that, when $p = 2$, system (4) models a continuous-time approximation of Nesterov's accelerated gradient method. However, while existing results have established convergence of (4) to solve optimization problems without plants in the loop, guaranteeing its convergence in the presence of plant dynamics is not trivial. Indeed, as recently shown in Hauswirth et al. (2020, Sec. IV.B) via numerical experiments, the interconnection between (4) and a dynamical plant can result in instabilities even when $k \to 0$. This observation finds a theoretical explanation through Poveda and Li (2019), where the authors show that for (4) no (strict) Lyapunov function exists due to absence of uniformity in the convergence (see Poveda and Li (2019, Prop. 1) and Poveda and Teel (2020, Thm. 1)). This prevents the direct application of standard singular perturbation tools (Khalil, 2002; Teel, Moreau, & Nesic, 2003) to establish closed-loop stability. To overcome these challenges, in this paper we introduce a new feedback controller that combines the continuous-time dynamics (4) with discrete-time periodic resets. We show that these hybrid controllers guarantee robust approximate tracking as well as acceleration properties. To the best of our knowledge, the results of this paper are the first that incorporate switching plants and hybrid controllers in online optimization.

2. Preliminaries and problem statement

Given a compact set $\mathcal{A} \subset \mathbb{R}^n$ and $x \in \mathbb{R}^n$, we define $|x|_{\mathcal{A}} := \min_{y\in\mathcal{A}} \|y - x\|_2$. When $\mathcal{A} = \{0\}$, $|x|_{\mathcal{A}} = |x|$ denotes the norm of x. Given $v \in \mathbb{R}^n$ and $w \in \mathbb{R}^m$, we let $(v, w) \in \mathbb{R}^{n+m}$ denote their concatenation. For a symmetric matrix $M \in \mathbb{R}^{n\times n}$, we let $\bar{\lambda}(M)$ and $\underline{\lambda}(M)$ denote its largest and smallest eigenvalues, respectively.

2.1. Set-valued hybrid dynamical systems

We use the framework of HDS to analyze switching systems and hybrid algorithms using a common mathematical framework. A HDS with state $\varphi \in \mathbb{R}^n$ and data (C, F, D, G), is given by

$$\varphi \in C, \ \dot{\varphi} \in F(\varphi), \qquad \varphi \in D, \ \varphi^+ \in G(\varphi), \tag{5}$$

where $F : \mathbb{R}^n \rightrightarrows \mathbb{R}^n$ and $G : \mathbb{R}^n \rightrightarrows \mathbb{R}^n$ are the flow and jump maps, respectively, whereas $C \subset \mathbb{R}^n$ and $D \subset \mathbb{R}^n$ are the flow and jump sets, respectively. System (5) generalizes continuous-time systems ($D = \varnothing$) and discrete-time systems ($C = \varnothing$). Solutions to (5) are parametrized by two time indices: a continuous index $t \in \mathbb{R}_{\geq 0}$ that increases continuously whenever the system flows in C as $\dot{\varphi}(t, j) := \frac{d}{dt}\varphi(t, j) \in F(\varphi(t, j))$; and a discrete index $j \in \mathbb{Z}_{\geq 0}$ that increases by one whenever the system jumps in D as $\varphi^+ := \varphi(t, j + 1) \in G(\varphi(t, j))$. Solutions to (5) are defined on hybrid time-domains (Goebel et al., 2012, Def. 2.3), namely, subsets of $\mathbb{R}_{\geq 0}\times\mathbb{Z}_{\geq 0}$ defined as the union of intervals $[t_j, t_{j+1}]\times\{j\}$, with $0 = t_0 \leq t_1 \leq \cdots$, and where the last interval can be closed or open on the right. In compact form, we denote by $\mathrm{dom}(\varphi)$ the domain of φ.

We study switching signals σ that satisfy an *average dwell-time* (ADT) condition (Hespanha & Morse, 1999) of the form $N(t, s) \leq N_0 + \frac{t-s}{\tau_d}$, $\forall\ 0 \leq s \leq t$, where $N(t, s)$ denotes the number of discontinuities of σ in the interval $(s, t]$, and $\tau_d > 0$ is the signal's dwell-time. The ADT condition guarantees that system (1) has at most N_0 switches at any time, and finitely-many switches in any finite time interval. As shown in Goebel et al. (2012, Ch. 2), HDS of the form (5) offer a mathematical model to capture any signal σ that satisfies the ADT condition: every switching signal σ satisfying ADT can be generated by a HDS with state $\chi = (\tau, \sigma) \in \mathbb{R}_{\geq 0} \times \mathcal{S}$, and data $(C_\chi, F_\chi, D_\chi, G_\chi)$:

$$\begin{aligned} C_\chi &:= [0, N_0] \times \mathcal{S}, \quad & F_\chi(\chi) &:= [0, \tau_d^{-1}] \times \{0\}, \\ D_\chi &:= [1, N_0] \times \mathcal{S}, \quad & G_\chi(\chi) &:= \{\tau - 1\} \times \mathcal{S}. \end{aligned} \tag{6}$$

Moreover, every signal σ generated by the HDS (6) has a hybrid time domain that satisfies the ADT condition.

2.2. Problem statement

We next formalize the problem of interest. For any fixed $u \in \mathbb{R}^m$, $\sigma \in \mathcal{S}$, and $\omega \in \mathbb{R}^q$, we write the steady-state output of (1) as: $y_\sigma = G_\sigma u + H_\sigma \omega$, where $G_\sigma := -CA_\sigma^{-1}B_\sigma$ and $H_\sigma := D - CA_\sigma^{-1}E_\sigma$. We will impose the following assumptions.

Assumption 1. For each $\sigma \in \mathcal{S}$, and each symmetric matrix $P_\sigma \succ 0$, there exists a unique symmetric matrix $Q_\sigma \succ 0$, such that $A_\sigma^T P_\sigma + P_\sigma A_\sigma = -Q_\sigma$.

Assumption 2. For each $\omega \in \mathbb{R}^q$ and each $u \in \mathbb{R}^m$ (constant), there exists a unique $x \in \mathbb{R}^n$, such that $A_\sigma x + B_\sigma u + E_\sigma \omega = 0$, for all $\sigma \in \mathcal{S}$.

Under Assumption 1, A_σ is Hurwitz and therefore invertible. On the other hand, Assumption 2 is common for the analysis of switched systems (Goebel et al., 2012; Hespanha & Morse, 1999) and it guarantees that all the modes have a common equilibrium (see also Remark 1), and that the input–output maps are common across the modes, i.e., $G := G_\sigma$ and $H := H_\sigma$ for all $\sigma \in \mathcal{S}$. Under these assumptions, we can rewrite (2) as:

$$\min_u \quad \phi_t(u) := \phi_u(u) + \phi_y(Gu + H\omega_t). \tag{7}$$

Here, the subscript t in $\phi_t(u)$ is used to emphasize the dependence on time in the cost due to ω_t. Note that every solution to (2) is a solution to (7), however, the inverse implication holds only when (A_σ, C_σ), $\sigma \in \mathcal{S}$, is observable. Since we will focus on (7), observability is not necessary in the subsequent analysis. For simplicity, we assume that for each $\omega_t \in \mathbb{R}^q$ problem (7) has a unique solution $u^*(\omega_t)$, and that the mapping $\omega_t \mapsto u_t^* := u^*(\omega_t)$ is smooth, with ω_t satisfying the following assumption.[1]

Assumption 3. The function $t \mapsto \omega_t$ is generated by an (unknown) Lipschitz continuous exosystem

$$\dot{\omega}_t = \Pi(\omega_t), \quad \omega_t \in \Gamma \subset \mathbb{R}^q, \tag{8}$$

with Γ being forward invariant and compact.

Assumption 3 is standard for regulation problems with exogenous inputs (see Gazi (2007) and Marconi and Teel (2010)), and it guarantees that $t \mapsto \omega_t$ is continuously differentiable and bounded.

Remark 1. When G_σ and H_σ are not common across modes, but all modes admit a common equilibrium point, we can define the average map $y = G_{\text{av}}u + H_{\text{av}}\omega_t$, where $G_{\text{av}} := \sum_{\sigma\in\mathcal{S}} \alpha_\sigma G_\sigma$ and $H_{\text{av}} := \sum_{\sigma\in\mathcal{S}} \alpha_\sigma H_\sigma$, with $0 \le \alpha_\sigma \le 1$, $\sum_\sigma \alpha_\sigma = 1$. In this case, (7) can be generalized to $\min_u \phi_u(u) + \phi_y(G_{\text{av}}u + H_{\text{av}}\omega_t)$. This scenario often emerges in transportation systems (Bianchin & Pasqualetti, 2020). □

In the remainder, we use $z := (x, u)$ for the joint state of the plant and the control signal, and $z_t^* := (x_t^*, u_t^*)$ to denote vectors that satisfy: $0 = A_\sigma x_t^* + B_\sigma u_t^* + E_\sigma \omega_t$, $\sigma \in \mathcal{S}$, and $0 = \nabla\phi_u(u_t^*) + G^T\nabla\phi_y(Gu_t^* + H\omega_t)$ at all times, where we use the notation $x_t^* := x^*(\omega_t)$. In words, the components of z_t^* correspond to equilibria of (1) and to time-varying optimizers of (7). The problem focus of this work is formalized next.

Problem 1. Let $\tilde{z} := z - z_t^*$ denote the tracking error. Design an output-feedback controller for (1) such that for any unknown exogenous signal $t \mapsto \omega_t$, the tracking error converges to a neighborhood of the origin, whose size is parameterized by the time-variation of ω_t, i.e., by $|\dot{\omega}_t|$. □

[1] In the next sections, and with some abuse of notation, we will use the shorthand notation u_t^* instead of $u^*(\omega_t)$. We will later drop this subscript in our stability analysis.

3. Main results

To address Problem 1, we propose two controllers: the first based on a gradient-flow method, and the second based on a hybrid accelerated gradient method.

3.1. Feedback control via online gradient descent

We first study the solution of the tracking Problem 1 via gradient-descent flows of the form (3). The left scheme of Fig. 1 illustrates the approach. For such systems, the following two assumptions are standard.

Assumption 4. The functions $\phi_u(\cdot)$ and $\phi_y(\cdot)$ are continuously differentiable, and their gradients are globally Lipschitz with constants $\ell_u > 0$ and $\ell_y > 0$, respectively.

Assumption 5. The function $u \mapsto \phi_t(u)$: (a) is radially unbounded for any $t \ge 0$, and (b) satisfies the Polyak-Łojasiewicz (PL) inequality, namely, $\exists\, \mu > 0$ such that $|\nabla\phi_t(u)|^2 \ge 2\mu(\phi_t(u) - \phi_t(u_t^*))$, for all $u \in \mathbb{R}^m$ and all $\omega_t \in \Gamma$.

Under Assumption 4, the mapping $u \mapsto \phi_t(u)$ has a globally Lipschitz gradient with Lipschitz constant $\ell := \ell_u + \ell_y|G|^2$. Similarly, Assumption 5 implies that $\phi_t(u) - \phi_t(u^*) \ge \frac{\mu}{2}|u - u_t^*|^2$, $\forall\, u \in \mathbb{R}^m$.

To design the controller, we note that if ω_t and H were known, the following dynamics can be shown to converge to u_t^* under Assumptions 4 and 5 (see, for example, Absil & Kurdyka, 2006):

$$\dot{u} = F_{GS}(u, \omega_t) := -\nabla\phi_u(u) - G^T\nabla\phi_y(Gu + H\omega_t). \tag{9}$$

When ω_t and H are unknown, we propose to approximate the steady-state output $Gu + H\omega_t$ with instantaneous feedback from the plant, leading to:

$$\dot{u} = F_G(u, y, \sigma) := -\eta_\sigma(\nabla\phi_u(u) + G^T\nabla\phi_y(y)), \tag{10}$$

where $\eta_\sigma > 0$ is a mode-dependent tunable gain.

The system obtained by interconnecting plant (1), the switching signal generator (6), and the controller (10) leads to a HDS of the form (5), denoted by $\mathcal{H}_G$, with state $\varphi = (x, u, \chi, \omega_t)$, continuous-time dynamics:

$$\begin{aligned} \dot{x} &= P_\sigma(x, u, \omega_t), & \dot{u} &= F_G(u, h(x, \omega_t), \sigma), \\ \dot{\chi} &\in F_\chi(\chi), & \dot{\omega}_t &= \Pi(\omega_t), \end{aligned} \tag{11}$$

flow set $C := \mathbb{R}^n \times \mathbb{R}^m \times C_\chi \times \Gamma$, discrete-time dynamics:

$$x^+ = x, \quad u^+ = u, \quad \chi^+ \in G_\chi(\chi), \quad \omega^+ = \omega, \tag{12}$$

and jump set $D := \mathbb{R}^n \times \mathbb{R}^m \times D_\chi \times \Gamma$.

Next, we provide a result that establishes an explicit tracking bound for (11). To this end, we require that the controller gain satisfies $0 < \eta_\sigma < \bar{\eta}_\sigma$, where

$$\bar{\eta}_\sigma = \frac{(1-\kappa)^2}{2-\kappa} \frac{\underline{\lambda}(Q_\sigma)}{\ell_y |C||G||P_\sigma A_\sigma^{-1} B_\sigma|}, \tag{13}$$

where (P_σ, Q_σ) are as in Assumption 1, and $\kappa \in (0, 1)$. Moreover, we define the following constants:

$$\theta_\sigma := \frac{1}{1 + 2|P_\sigma A_\sigma^{-1} B_\sigma|}, \tag{14a}$$

$$\bar{a}_\sigma := \frac{1}{\eta} \max\left\{(1-\theta_\sigma)\frac{\ell}{2}, \theta_\sigma \bar{\lambda}(P_\sigma)\right\}, \tag{14b}$$

$$\underline{a}_\sigma := \frac{1}{\eta} \min\left\{(1-\theta_\sigma)\frac{\mu}{2}, \theta_\sigma \underline{\lambda}(P_\sigma)\right\}, \tag{14c}$$

$$b_\sigma = \frac{\kappa}{2} \min\left\{2\mu\eta_\sigma, \frac{\underline{\lambda}(Q_\sigma)}{\bar{\lambda}(P_\sigma)}\right\}, \tag{14d}$$

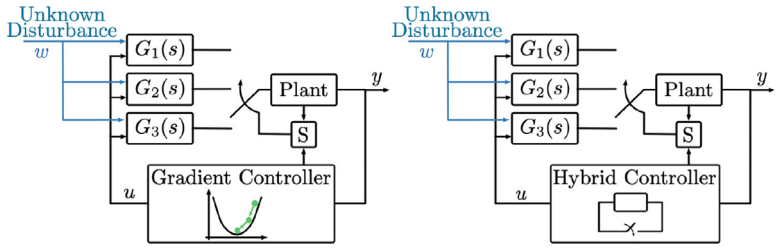

Fig. 1. (left) A switched system in feedback with a gradient flow controller. (right) A switched system in feedback with a hybrid controller. "S" denotes a supervisory controller that actuates the switching between the modes of the plant.

$$d_\sigma = \frac{2}{\kappa}\max\left\{\frac{\ell_y|H||G|}{\eta_\sigma\mu^2}, \frac{2|P_\sigma A_\sigma^{-1}E_\sigma|}{\underline{\lambda}(Q_\sigma)}\right\}, \tag{14e}$$

where $(\mu, \ell, \ell_y, \ell_u)$ are as in Assumptions 4 and 5.

Theorem 3.1. *Suppose that Assumptions 1–5 hold. If $\eta_\sigma \in (0, \bar{\eta}_\sigma)$ for all $\sigma \in \mathcal{S}$ and the dwell-time satisfies $\tau_d > \frac{\ln a}{\min_\sigma b_\sigma}$, then the tracking error $\tilde{z} = z - z_t^*$ of the system $\mathcal{H}_G$ satisfies:*

$$|\tilde{z}(t,j)| \le a_0 e^{-\frac{b_0 t + c_0 j}{2}}|\tilde{z}(0,0)| + a_0 d_0 \sup_{0\le\tau\le t}|\dot{\omega}_\tau|, \tag{15}$$

where $a_0 = e^{\frac{\varrho}{2}N_0}\sqrt{a}$, $b_0 = \min_\sigma b_\sigma - \frac{\varrho}{\tau_d}$, $c_0 = \varrho - \ln a$, $d_0 = \max_\sigma d_\sigma$, with $a := \frac{\max_\sigma \bar{a}_\sigma}{\min_\sigma \underline{a}_\sigma}$ and $\varrho > 0$ is any constant that satisfies $\ln a < \varrho < \tau_d \min_\sigma b_\sigma$. □

This result establishes that a sufficiently-small gain η_σ guarantees exponential convergence of z to a neighborhood of the optimal trajectory z_t^*. As characterized by (13), the upper bound on the controller gain is proportional to the rate of convergence of the open-loop plant $\underline{\lambda}(Q_\sigma)/\bar{\lambda}(P_\sigma)$, and inversely proportional to the Lipschitz constant of the cost function ℓ_y. Moreover, as characterized by (14d), the rate of decay of the tracking error is governed by the minimum between the rate of convergence of the controller (namely, $2\mu\eta_\sigma$) and the rate of convergence of the plant (namely, $\underline{\lambda}(Q_\sigma)/\bar{\lambda}(P_\sigma)$).

Remark 2. The constants (a_0, b_0, c_0, d_0) characterized in Theorem 3.1 depend on: (i) (μ, ℓ), which characterize the smoothness and gradient dominance of the *steady state* cost function (7); (ii) the matrices $(A_\sigma, B_\sigma, C, D, E_\sigma)$ and (Q_σ, P_σ), which govern the dynamics of the switched plant (1); and (iii) (τ_d, N_0) that govern the behavior of the signal σ in (6). □

Remark 3. Assumption 5 is fundamental to guarantee exponential convergence. Indeed, as $\mu \to 0$, we have that $b_\sigma \to 0$ and $d_\sigma \to \infty$. Similar scenarios were recently investigated in Menta et al. (2018) and Hauswirth et al. (2020). In contrast to these results, Theorem 3.1 accounts for *time-varying* disturbances, *switching* plant dynamics, and establishes an explicit *exponential* bound, as opposed to asymptotic convergence. □

3.2. Feedback control via hybrid gradient descent

We now address Problem 1 by proposing a feedback controller inspired by the accelerated gradient method (4). To design the controller, we adapt (4) as follows: first we rewrite (4) as a set of first-order ODEs by letting $p = 2$ and by defining the variables $u_1 := u$ and $u_2 := \frac{\tau}{2}\dot{u}_1 + u_1$; second, we introduce an auxiliary state u_3 that models the evolution of a timer and replaces the temporal variable τ, thus leading to the dynamics:

$$\dot{u}_1 = \frac{2}{u_3}(u_2 - u_1), \tag{16a}$$

$$\dot{u}_2 = -2ku_3\left(\nabla\phi_u(u_1) + G^\mathsf{T}\nabla\phi_y(Gu_1 + H\omega_t)\right), \tag{16b}$$

$$\dot{u}_3 = \frac{1}{2}. \tag{16c}$$

The choice of the variables (u_1, u_2, u_3) is inspired by accelerated momentum-based optimization and estimation algorithms proposed in e.g. Gaudio et al. (2021), Poveda and Li (2021), and Wibisono et al. (2016, Eq. (14)). We note that the choice $\dot{u}_3 = 1/2$, also used in Poveda and Li (2021) to solve *static* optimization problems, is motivated by our Lyapunov-based analysis.

Remark 4. As shown in Poveda and Li (2019, Prop. 1) and Poveda and Teel (2020, Thm.1), the convergence of (16) lacks uniformity with respect to the initial value of u_3. In turn, this precludes the application of standard multi-time scale techniques using quadratic-type Lyapunov functions (Khalil, 2002, pp. 453) or regular perturbations techniques, see Teel et al. (2003, Thm. 1). □

Similar to (9), the dynamics (16) require knowledge of H and ω_t to be implemented. Hence, we propose to approximate the steady-state output $Gu_1 + H\omega_t$ with the instantaneous output y of the dynamical system. While this modification leads to an accelerated version of the controller proposed in Section 3.1, empirical and theoretical evidence suggests that such modifications are not sufficient to guarantee tracking of the optimal trajectories (see Remark 4). To address this limitation, we introduce discrete-time resets of the state variables of (16), which resemble the "restarting" heuristics used in the literature of machine learning (O'Donoghue & Candes, 2015; Su et al., 2014; Wibisono et al., 2016) and hybrid control (Prieur, Queinnec, Tarbouriech, & Zaccarian, 2018). The proposed controller is then hybrid, with state $u = (u_1, u_2, u_3)$, continuous-time dynamics

$$\dot{u} = F_H(u, y, \sigma) := \eta_\sigma \begin{pmatrix} \frac{2}{u_3}(u_2 - u_1) \\ -2ku_3\left(\nabla\phi_u(u_1) + G^\mathsf{T}\nabla\phi_y(y)\right) \\ \frac{1}{2} \end{pmatrix},$$

where $\eta_\sigma > 0$ is a mode-dependent tunable gain; flow set $C_H = \mathbb{R}^n \times \mathbb{R}^n \times [\delta, \Delta]$, where $\Delta > \delta > 0$ are tunable parameters characterizing the restarts of the timer variable; discrete-time dynamics

$$u^+ = G_H(u) := R_0 u, \quad R_0 = \begin{bmatrix} I & 0 & 0 \\ r_0 I & (1-r_0)I & 0 \\ 0 & 0 & \frac{\delta}{\Delta} \end{bmatrix},$$

where $r_0 \in \{0, 1\}$ is a design parameter describing the *reset policy*; and jump set $D_H = \mathbb{R}^n \times \mathbb{R}^n \times \{\Delta\}$.

The rationale behind the controller is as follows: when the timer u_3 is equal to Δ, the controller states (u_1, u_2) are re-initialized and the timer variable is reset to the value δ. When $r_0 = 0$, only the timer u_3 is reset to δ, whereas when $r_0 = 1$ both the momentum variable u_2 is re-initialized to u_1, and the timer u_3 is reset to δ. By recalling the definition of u_2, we notice that the latter restarting policy corresponds to setting $\dot{u}_1$ to zero.

The interconnection of the hybrid controller and the switched LTI plant (1) leads to a HDS with state $\varphi = (x, u, \chi, \omega_t)$, continuous-time dynamics:

$$\begin{aligned} \dot{x} &= P_\sigma(x, u, \omega_t), & \dot{u} &= F_H(u, h(x, \omega_t), \sigma), \\ \dot{\chi} &\in F_\chi(\chi), & \dot{\omega}_t &= \Pi(\omega_t), \end{aligned} \tag{17}$$

and flow set $C = \mathbb{R}^n \times C_H \times C_\chi \times \Gamma$. Jumps in the closed-loop system can be triggered by both switches of the plant and by resets of the controller. Therefore, the discrete-time dynamics are captured by the inclusion:

$$\varphi \in D := D_1 \cup D_2, \quad \varphi^+ \in G(\varphi), \tag{18}$$

where the set-valued map G and the sets D_1, D_2 are

$$G(\varphi) := \begin{cases} G_1(\varphi), & \varphi \in D_1 := \mathbb{R}^n \times C_H \times D_\chi \times \Gamma, \\ G_2(\varphi), & \varphi \in D_2 := \mathbb{R}^n \times D_H \times C_\chi \times \Gamma, \\ G_1(\varphi) \cup G_2(\varphi), & \varphi \in D_1 \cap D_2, \end{cases} \tag{19}$$

with $G_1(\varphi) := \{x\} \times \{u\} \times G_\chi(\chi) \times \{\omega_t\}$ and $G_2(\varphi) := \{x\} \times \{G_H(u)\} \times \{\chi\} \times \{\omega_t\}$. We denote the hybrid system (17)–(19) in compact form by $\mathcal{H}_H$.

Remark 5. Notice that the model (17)–(19) naturally captures non-uniqueness of solutions that can emerge when the plant and the controller are in their jump sets simultaneously. In these scenarios, arbitrarily-small disturbances may force the plant or the controller to jump before the other, and a well-posed model of the hybrid dynamics allows us to capture both behaviors of the system as the disturbance vanishes. □

Next, we provide error-tracking guarantees for $\mathcal{H}_H$. To this end, we first consider the case where the disturbance ω_t is constant, and we show that the (time-invariant) optimizer is globally practically asymptotically stable.

Remark 6. Since we first focus on asymptotic stability properties, it suffices to consider plants (1) with a single mode (i.e., $\mathcal{S} := \{\sigma\}$). Indeed, if each individual mode in $\mathcal{S}$ leads to asymptotic stability of the closed-loop system, then semi-global practical asymptotic stability (with respect to τ_d^{-1} in (6)) for the system with multiple modes will follow directly from Goebel et al. (2012, Corollary 7.28). □

We begin by introducing an inverse Lipschitz-type assumption.

Assumption 6. The function $u \mapsto \phi_t(u)$ is convex, radially unbounded, and for each $\nu_0 > 0$ there exists $\ell_0 > 0$ such that $|u - u_t^*| \geq \nu_0$ for some $u \in \mathbb{R}^m$ implies $|\nabla \phi_t(u)| \geq \ell_0 |u - u_t^*|$. □

Next, we require that the controller gain satisfies $0 < \eta_\sigma < \bar{\eta}_\sigma$, where

$$\bar{\eta}_H = \frac{\underline{\lambda}(Q_\sigma)}{2\ell_y |C||G|} \min\left\{ \frac{1}{2k\delta\Delta |P_\sigma A_\sigma^{-1} B_\sigma|}, \frac{\theta \ell_0^2 \delta \kappa^2 k}{2(1-\theta)\ell\Delta |C||G|} \right\}.$$

with $\kappa \in (0, 1)$ and

$$\theta = \frac{\ell_y k \Delta |C||G|}{\ell_y k \Delta |C||G| + 2\delta |P_\sigma A_\sigma^{-1} B_\sigma|}.$$

Using this gain, we obtain the following result:

Theorem 3.2. *Let Assumptions 1–4 and 6 hold, and assume that $\omega_t := \omega \in \mathbb{R}^q$ is constant, that the plant has a single mode $\mathcal{S} = \{\sigma\}$, and let the reset policy be $r_0 = 0$. If $\eta_\sigma \in (0, \bar{\eta}_\sigma)$, then any solution of $\mathcal{H}_H$ satisfies:*

$$(a)\ \limsup_{t+j\to\infty} |z(t,j) - z^*| \leq \nu_0, \qquad \forall (t,j) \in dom(\varphi).$$

$$(b)\ \phi(u_1(t,j)) - \phi(u^*) \leq \frac{\alpha_j}{u_3^2(t,j)} + \nu_0,\ \forall (t,j) \in dom(\varphi), t > \underline{t}_j,$$

where $\alpha_j > 0$, $z := (x, u_1)$, $z^* := (x^*, u^*)$, and $\underline{t}_j := \min\{t \geq 0 : (t,j) \in dom(\varphi)\}$. □

The convergence result of Theorem 3.2 is global, but of "practical" nature. Namely, convergence is achieved only to a ν_0-neighborhood of the optimal set via the choice of $\bar{\eta}_\sigma$, which, in turn, depends on the constant ℓ_0. Two main comments are in order. First, the upper bound on the controller gain $\bar{\eta}_\sigma$ shrinks to zero when either $\delta \to 0^+$ or $\Delta \to \infty$. Since $\delta = 0$ and $\Delta = \infty$ correspond to the (non-restarted) ODE (4), our analysis suggests that for (4) there may not exist a gain $\eta > 0$ that guarantees stability for the closed-loop system: a similar observation was recently made in Hauswirth et al. (2020, Sec. IV.B). Second, the result establishes that the error in the *steady-state* cost function decreases (outside a neighborhood of the optimal point) at a rate of order $\mathcal{O}(c_j/u_3^2)$ during the jth interval of flow, where c_j is constant in each interval. Thus, the larger the difference $\Delta - \delta$, the larger the size of the intervals where this bound holds. This can be seen as a semi-acceleration property that holds during flows. Indeed, using the definition of u_3, during the first interval of flow we have that $u_3(t, 0) = u_3(0, 0) + 0.5t$, and the error in the cost decreases at a rate $\mathcal{O}(c_0/t^2)$; see also Poveda and Li (2021), Su et al. (2014) and Wibisono et al. (2016) for similar bounds in static optimization problems. We also note that, as revealed by the proof (presented below), and in contrast to the case of optimization problems without plants in the loop, the quantity α_j in item *(b)* explicitly depends on the LTI plant (1) via the matrix P_σ. Finally, we note that as $\nu_0 \to 0$, the controller gain might satisfy $\eta \to 0$, as shown in the following example.

Example 1. Let $\phi(u_1) = \frac{1}{\theta}(|u_1 - u^*|^\theta + |Gu_1 + H\omega_t|^\theta)$, with $\theta \in \mathbb{Z}_{\geq 2}$, which is not strongly convex when $\theta > 2$. Also, let $G = [g_{ij}]$ with $g_{ij} \geq 0$ for all i, j, as it is the case in compartmental systems (Bianchin & Pasqualetti, 2020). It then follows that $|\nabla \phi(u_1)| \geq |u_1 - u_t^*|^{\theta-1} \geq \nu_0^{\theta-2} |u_1 - u_t^*|$. Thus, ϕ_t satisfies Assumption 6 with $\ell_0 = \nu_0^{\theta-2}$. Note that in this case, as $\nu_0 \to 0^+$, the admissible constant ℓ_0 and the controller gain $\bar{\eta}_\sigma$ shrink to zero. This relation suggests that as the size of the neighborhood satisfies $\nu_0 \to 0$, the controller gain also satisfies $\eta \to 0$. □

Next, under the following strong convexity assumption, we will show that the hybrid controller can solve Problem 1 with an exponential rate of convergence.

Assumption 7. There exists $\mu \in \mathbb{R}_{>0}$ such that $\phi_t(u) \geq \phi_t(u') + \nabla \phi_t(u')^\intercal (u - u') + \frac{\mu}{2} |u - u'|^2$ holds for all $u, u' \in \mathbb{R}^m$, and all $\omega_t \in \Gamma$.

To establish an exponential tracking bound, we require that the controller gain satisfies $\eta_\sigma < \bar{\eta}_\sigma$, where

$$\bar{\eta}_\sigma = \frac{(1-\kappa)^2}{16} \frac{\delta \underline{\lambda}(Q_\sigma)}{k\Delta \ell_y |C||G||P_\sigma A_\sigma^{-1} B_\sigma|}, \quad \kappa \in (0, 1). \tag{20}$$

Moreover, we define the following constants:

$$\theta_\sigma = \frac{k\Delta \ell_y |C||G|}{k\Delta \ell_y |C||G| + 2\delta^{-1} |P_\sigma A_\sigma^{-1} B_\sigma|}, \tag{21a}$$

$$\bar{a}_\sigma := \max\left\{(1-\theta_\sigma)\frac{1+k\ell\Delta^2}{2}, \theta_\sigma\bar{\lambda}(P_\sigma)\right\}, \tag{21b}$$

$$\underline{a}_\sigma := \min\left\{(1-\theta_\sigma)\frac{1+2k\ell\Delta^2}{4}, \theta_\sigma\underline{\lambda}(P_\sigma)\right\}, \tag{21c}$$

$$b_\sigma = \frac{\kappa}{2}\min\left\{\frac{2\eta_\sigma}{\Delta(1+2k\ell\Delta^2)}, \frac{\eta_\sigma k\delta\mu}{2(1+2k\ell\Delta^2)}, \frac{\underline{\lambda}(Q_\sigma)}{\bar{\lambda}(P_\sigma)}\right\}, \tag{21d}$$

$$d_\sigma = \frac{2}{\kappa}\max\left\{\frac{\bar{d}_\sigma}{\eta_\sigma\min\{\Delta^{-1}, k\delta\mu/4\}}, \frac{2|P_\sigma A_\sigma^{-1}E_\sigma|}{\underline{\lambda}(Q_\sigma)}\right\}. \tag{21e}$$

where $\bar{d}_\sigma := \sqrt{2}k\Delta^2\ell_y|H||G| + \sqrt{2}\max_{\omega\in\Gamma}|\frac{\partial u^*}{\partial\omega}|(k\Delta^2 + \frac{1}{2}(1+2k\Delta^2\ell))$.

Theorem 3.3. *Let Assumptions 1–4 and 7 hold and let the reset policy be $r_0 = 1$. If $\eta_\sigma \in (0, \bar{\eta}_\sigma)$ for all $\sigma \in \mathcal{S}$, the timer thresholds satisfy $\Delta^2 - \delta^2 > \frac{1}{2k\mu}$, and the dwell-time satisfies $\tau_d > \frac{\ln a}{\min_\sigma b_\sigma}$, then the tracking error $\tilde{z} = z - z_t^*$ of the system $\mathcal{H}_H$ satisfies:*

$$|\tilde{z}(t,j)| \le a_0 e^{-\frac{b_0 t + c_0 j}{2}}|\tilde{z}(0,0)| + a_0 d_0 \sup_{0\le\tau\le t}|\dot{\omega}_\tau|, \tag{22}$$

where $a_0 = e^{\frac{\varrho}{2}N_0}\sqrt{a}$, $b_0 = \min_\sigma b_\sigma - \frac{\varrho}{\tau_d}$, $c_0 = \varrho - \ln a$, $d_0 = \max_\sigma d_\sigma$, with $a := \frac{\max_\sigma \bar{a}_\sigma}{\min_\sigma \underline{a}_\sigma}$ and $\varrho > 0$ is any constant that satisfies $\ln a < \varrho < \tau_d \min_\sigma b_\sigma$. □

The result of Theorem 3.3 requires three types of conditions on the controller parameters: (i) a sufficiently-small choice of the controller gain η_σ, (ii) a quadratic-like dwell-time condition $\Delta^2 - \delta^2 > 1/2k\mu$, which gives a lower bound on the restarting frequency, and (iii) an average dwell-time condition on the switching signal σ.

Remark 7. The controller used in Theorem 3.3 leverages resets of the momentum variable. Similar "restarting" techniques have been studied in literature of optimization and machine learning (Su et al., 2014; Wibisono et al., 2016), with optimal restarting frequencies presented in O'Donoghue and Candes (2015, Thm. 3.1) and Poveda and Li (2021, Sec.3.2.1). For example, in Poveda and Li (2021, Sec. 3.2.1), it is shown that, as $\delta \to 0^+$, the choice $\Delta = e\sqrt{\frac{1}{2k\mu} + \delta^2}$ with $k = 1/2\ell$ can achieve exponential convergence of order $\mathcal{O}(e^{-t\sqrt{\mu/\ell}})$. This is particularly advantageous in problems with condition numbers satisfying $\ell/\mu \gg 1$. In the context of feedback-based optimization, the advantages of using momentum are recovered as the time scale separation between the plant and the controller increases. Numerical experiments are presented in Section 5. □

We conclude by noting that the closed-loop systems $\mathcal{H}_H$ with constant disturbances $\omega_t = \omega$ are robust to *small bounded additive* disturbances $t \mapsto e(t)$ acting on the states and dynamics of the system. Indeed, by construction, the hybrid system $\mathcal{H}_H$ is well-posed and it satisfies the Basic Conditions (Goebel et al., 2012, Assump. 6.5). Therefore, the robustness property follows directly by Goebel et al. (2012, Cor. 7.27).

4. Proofs

To prove our main results, we use tools from HDS theory (Goebel et al., 2012). We model the closed-loop system as a time-invariant and well-posed HDS described by the interconnection between the plant (1), the switching generator (6), the exosystem (8), and the controller. For this interconnection, we construct a hybrid Lyapunov function to guarantee stability of the closed-loop dynamics. The construction of the Lyapunov function is inspired by singular perturbation arguments (Khalil, 2002), adjusted to account for the switching dynamics and the hybrid controllers. This construction allows us to derive conditions on η_σ and on the dwell-time parameters of σ to guarantee suitable asymptotic or exponential input-to-state stability with respect to $|\dot{\omega}|$. Since the closed-loop system can be modeled as a time-invariant HDS, in our analysis we drop the subscript t from the signal ω, the optimizer $u^*(\omega)$, and the cost function (7), which we write as an explicit function of u and ω, of the form $\phi(u,\omega)$.

4.1. Proof of Theorem 3.1

We divide the proof into four main steps.

Step 1. Consider the change of variable $\tilde{u} := u - u^*(\omega)$, and $\tilde{x} := x - \left(-A_\sigma^{-1}B_\sigma(\tilde{u} + u^*(\omega)) - A_\sigma^{-1}E_\sigma\omega\right)$, which denote the tracking error of the plant and the controller, respectively. The dynamics of $\tilde{u}$ are:

$$\begin{aligned}\dot{\tilde{u}} &= \dot{u} - \dot{\overbrace{u^*(\omega)}} = -\eta\Big(\nabla\phi_u(\tilde{u} + u^*(\omega)) \\ &\quad + G^\top\nabla\phi_y\big(C\tilde{x} + G(\tilde{u} + u^*(\omega)) + H\omega\big)\Big) - \dot{\overbrace{u^*(\omega)}} \\ &=: \eta\psi_c(\tilde{x},\tilde{u},\omega) - \dot{\overbrace{u^*(\omega)}},\end{aligned} \tag{23}$$

and note that $\psi_c(0,\tilde{u},\omega) = -\nabla_u\phi(\tilde{u} + u^*(\omega),\omega)$. Also

$$\dot{\tilde{x}} = A_\sigma\tilde{x} + \eta A_\sigma^{-1}B_\sigma\psi_c(\tilde{x},\tilde{u},\omega) + A_\sigma^{-1}E_\sigma\dot{\omega}. \tag{24}$$

Next, we consider the Lyapunov-like function

$$V_\sigma(\tilde{z},\omega) = \frac{(1-\theta_\sigma)}{\eta}V_1(\tilde{u},\omega) + \frac{\theta_\sigma}{\eta}V_2(\tilde{x},\sigma), \tag{25}$$

with $\tilde{z} = (\tilde{x},\tilde{u})$, $\theta_\sigma \in (0,1)$ is as in (14), and $V_1(\tilde{u},\omega) := \phi_t(\tilde{u} + u^*(\omega),\omega) - \phi_t(u^*(\omega),\omega)$, $V_2(\tilde{x},\sigma) := \tilde{x}^\top P_\sigma\tilde{x}$, with P_σ given by Assumption 1. The function V_σ is a convex combination of a Lyapunov function for a linear plant and a Lyapunov function for a gradient-type ODE. By Assumption 1, we have that $\underline{\lambda}(P_\sigma)|\tilde{x}|^2 \le V_2(\tilde{x}) \le \bar{\lambda}(P_\sigma)|\tilde{x}|^2$. Also, by Assumptions 4 and 5, we have that $\frac{\mu}{2}|\tilde{u}|^2 \le V_1(\tilde{u},\omega) \le \frac{\ell}{2}|\tilde{u}|^2$, for all $\omega \in \Gamma$. Therefore, $\underline{a}|\tilde{z}_\sigma|^2 \le V_\sigma(\tilde{z},\omega) \le \bar{a}_\sigma|z|^2$, for all $\omega \in \Gamma$, with $\bar{a}_\sigma$ and $\underline{a}_\sigma$ given by (14b) and (14c).

Step 2. Next, we show that for each fixed mode $\sigma \in \mathcal{S}$, and outside a neighborhood of the origin that is proportional in size to $|\dot{\omega}|$, the function V_σ decreases along the trajectories of (23) and (24) at an exponential rate. In particular, note that

$$\begin{aligned}\frac{1}{\eta}\nabla_{\tilde{u}}V_1^\top\dot{\tilde{u}} &= -\psi_c(0,\tilde{u},\omega)^\top\Big(\psi_c(\tilde{x},\tilde{u},\omega) - \frac{1}{\eta}\dot{\overbrace{u^*(\omega)}}\Big) \\ &\le -|\psi_c(0,\tilde{u},\omega)|^2 + a_2|\psi_c(0,\tilde{u},\omega)||\tilde{x}| \\ &\quad + \frac{1}{\eta}\psi_c(0,\tilde{u},\omega)^\top\frac{\partial u^*}{\partial\omega}\dot{\omega},\end{aligned}$$

where the last inequality follows by Assumption 4 with $a_2 := \ell_y|C||G|$. Similarly, we have that

$$\nabla_\omega V_1^\top\dot{\omega} = \big(\nabla_\omega\phi(\tilde{u} + u^*(\omega),\omega) - \nabla_\omega\phi(u^*(\omega),\omega)\big)^\top\dot{\omega}. \tag{26}$$

Using the structure of ϕ_t, and the chain rule:

$$\begin{aligned}\nabla_\omega\phi_t &= \frac{\partial u^*}{\partial\omega}^\top\nabla\phi_u + H^\top\nabla\phi_y + \frac{\partial u^*}{\partial\omega}^\top G^\top\nabla\phi_y \\ &= \frac{\partial u^*}{\partial\omega}^\top\nabla_u\phi + H^\top\nabla\phi_y.\end{aligned} \tag{27}$$

Since $\nabla_u\phi_t(u^*(\omega)) = 0$, and using the definition of $\psi_c(0,\tilde{u},\omega)$, it follows that

$$\nabla_\omega V_1^\top\dot{\omega} \le -\left(\frac{\partial u^*}{\partial\omega}^\top\psi_c(0,\tilde{u},\omega)\right)^\top\dot{\omega} + \ell_y|H|\,|G|\,|\tilde{u}|\,|\dot{\omega}|.$$

where we used again Assumption 4. Since $\dot{V}_1 = \nabla_{\tilde{u}} V_1^\top \dot{\tilde{u}} + \nabla_\omega V_1^\top \dot{\omega}$, we have

$$\begin{aligned}\frac{1}{\eta}\dot{V}_1 &\leq -|\psi_c(0,\tilde{u},\omega)|^2 + a_2|\psi_c(0,\tilde{u},\omega)||\tilde{x}| \\ &\quad + \frac{1}{\eta}\psi_c(0,\tilde{u},\omega)^\top \frac{\partial u^*}{\partial \omega}\dot{\omega} - \frac{1}{\eta}\left(\frac{\partial u^*}{\partial \omega}^\top \psi_c(0,\tilde{u},\omega)\right)^\top \dot{\omega} \\ &\quad + \frac{\ell_y}{\eta}|H|\,|G|\frac{|\psi_c(0,\tilde{u},\omega)|}{\mu}|\dot{\omega}| \\ &\leq -|\psi_c(0,\tilde{u},\omega)|^2 + a_2|\psi_c(0,\tilde{u},\omega)||\tilde{x}| \\ &\quad + \frac{\ell_y}{\eta\mu}|H|\,|G|\,|\psi_c(0,\tilde{u},\omega)|\,|\dot{\omega}|,\end{aligned}$$

where the last term follows from the quadratic growth inequality. Using $|\nabla_u \phi_t|^2 \geq 2\mu V_1$, we obtain:

$$\frac{1}{\eta}\dot{V}_1 \leq -a_1|\psi_c(0,\tilde{u},\omega)|^2 + a_2|\psi_c(0,\tilde{u},\omega)||\tilde{x}| - a_3 V_1(\tilde{u},\omega),$$

where $a_1 = (1-\kappa)$ and $a_3 = \kappa\mu$, which holds whenever $|\psi_c(0,\tilde{u},\omega)| \geq \frac{2\ell_y|H||G|}{\kappa\eta\mu}|\dot{\omega}|$. Since $|\psi_c(0,\tilde{u},\omega)| \geq \mu|\tilde{u}|$, a sufficient condition for the above inequality to hold is $|\tilde{u}| \geq \frac{2\ell_y|H||G|}{\kappa\eta\mu^2}|\dot{\omega}|$.

On the other hand, for each fixed $\sigma \in \mathcal{S}$, we have:

$$\begin{aligned}\frac{1}{\eta}\dot{V}_2 &= 2\tilde{x}^\mathsf{T} P_\sigma\left(\frac{1}{\eta}A_\sigma\tilde{x} + A_\sigma^{-1}B_\sigma\psi_c(\tilde{x},\tilde{u},\omega) + \frac{1}{\eta}A_\sigma^{-1}E_\sigma\dot{\omega}\right) \\ &\leq -\frac{\underline{\lambda}(Q_\sigma)}{\eta}|\tilde{x}|^2 + 2|P_\sigma A_\sigma^{-1}B_\sigma||\tilde{x}||\psi_c(\tilde{x},\tilde{u},\omega)| \\ &\quad + \frac{2}{\eta}|P_\sigma A_\sigma^{-1}E_\sigma||\tilde{x}||\dot{\omega}|, \qquad (28)\end{aligned}$$

where the inequality follows from Assumption 1. Since $|\psi_c(\tilde{x},\tilde{u},\omega)| \leq |\psi_c(0,\tilde{u},\omega)| + a_2|\tilde{x}|$, and $V_2(\tilde{x},\sigma) \leq \bar{\lambda}(P_\sigma)|\tilde{x}|^2$, we can further upper bound (28) as:

$$\frac{1}{\eta}\dot{V}_2 \leq -\frac{b_1}{\eta}|\tilde{x}|^2 + b_2|\tilde{x}||\psi_c(0,\tilde{u},\omega)| + b_3|\tilde{x}|^2 - b_4 V_2(\tilde{x},\sigma),$$

which holds whenever $|\tilde{x}| \geq \frac{4|P_\sigma A_\sigma^{-1}E_\sigma|}{\kappa\underline{\lambda}(Q_\sigma)}|\dot{\omega}|$, where $b_1 := (1-\kappa)\underline{\lambda}(Q_\sigma)$, $b_2 := 2|P_\sigma A_\sigma^{-1}B_\sigma|$, $b_3 := 2a_2|P_\sigma A_\sigma^{-1}B_\sigma|$, and $b_4 := \frac{\kappa}{2\eta}\frac{\underline{\lambda}(Q_\sigma)}{\bar{\lambda}(P_\sigma)}$.

Step 3. Next, using the bounds on $\dot{V}_1$ and $\dot{V}_2$, we obtain that for each fixed $\sigma \in \mathcal{S}$ the function V_σ satisfies the following bound outside a $|\dot{\omega}|$-neighborhood of the origin:

$$\dot{V}_\sigma \leq -\xi^\mathsf{T}\Lambda_\sigma\xi - \frac{\kappa}{2}\min\left\{2\eta\mu, \frac{\underline{\lambda}(Q_\sigma)}{\bar{\lambda}(P_\sigma)}\right\}V_\sigma(\tilde{z},\omega), \qquad (29)$$

where $\xi = (|\nabla\phi(\tilde{u}+u^*(\omega),\omega)|, |\tilde{x}|)$ and Λ_σ is a 2×2 symmetric matrix with entries $\Lambda_{11} = (1-\theta)a_1$, $\Lambda_{12} = \Lambda_{12} = -\frac{1}{2}((1-\theta)a_2 + \theta b_2)$, and $\Lambda_{22} = \theta(b_1/\eta - b_3)$. Since the largest $\theta \in (0,1)$ that guarantees $\Lambda \succ 0$ is as in (14), we conclude that $\Lambda \succ 0$ when $\eta_\sigma \in (0, \bar{\eta}_\sigma)$, with $\bar{\eta}_\sigma$ as in (13).

Step 4. Finally, we incorporate the switches of the plant which are governed by the states (σ,τ) generated by (6). Using V_σ, we consider the extended function $W(\tilde{\vartheta}) = e^{\varrho\tau}V_\sigma(\tilde{z},\omega)$, where $\varrho > 0$ and $\tilde{\vartheta} := (\tilde{z},\sigma,\tau,\omega)$. We will show the existence of ϱ such that W is a hybrid ISS Lyapunov function for the HDS with dynamics (6), (8), and (23)–(24), with respect to the "input" $|\dot{\omega}|$, and the compact set $\mathcal{A}_1 := \{\tilde{\vartheta} : \tilde{z} = 0,\ \sigma \in \mathcal{S},\ \tau \in [0,N_0],\ \omega \in \Gamma\}$. Indeed, note that for all $\tilde{z} \in \mathbb{R}^{n+m}$, all $(\tau,\sigma) \in [0,N_0]\times\mathcal{S}$, and $\omega \in \Gamma$, we have that $\min_\sigma \underline{a}_\sigma|\tilde{z}|^2 \leq W(\tilde{\vartheta}) \leq e^{\varrho N_0}\max_\sigma \bar{a}_\sigma|\tilde{z}|^2$, where $\underline{a}_\sigma, \bar{a}_\sigma$ are as in (14). During flows, we have that:

$$\dot{W} = e^{\varrho\tau}(\varrho V_\sigma\dot{\tau} + \dot{V}_\sigma) \leq \left(\frac{\varrho}{\tau_d} - \min_\sigma b_\sigma\right)W(\tilde{\vartheta}),$$

where b_σ is as in (14d), which holds whenever $|\tilde{u}| \geq \frac{2\ell_y|H||G|}{\kappa\eta\mu^2}|\dot{\omega}|$ and $|\tilde{x}| \geq \frac{4|P_\sigma A_\sigma^{-1}E_\sigma|}{\kappa\underline{\lambda}(Q_\sigma)}|\dot{\omega}|$. Hence, W decreases during flows if $\varrho < \tau_d \min_\sigma b_\sigma$. Next, note that at each jump we have that $\tilde{x}^+ = \tilde{x}$, $\tilde{u}^+ = \tilde{u}$, $\sigma^+ \in \mathcal{S}$, $\omega^+ = \omega$, and $\tau^+ = \tau - 1$. Hence, $W(\tilde{\vartheta}^+) \leq e^{\varrho\tau^+}\max_\sigma V_\sigma(\tilde{z}^+,\omega^+)$ and $W(\tilde{\vartheta}^+) \leq e^{-\varrho+\ln(\max_\sigma \bar{a}_\sigma)-\ln(\min_\sigma \underline{a}_\sigma)}W(\tilde{\vartheta})$. It follows that if $\varrho > \ln\left(\max_\sigma \bar{a}_\sigma / \min_\sigma \underline{a}_\sigma\right)$, the function W also decreases during jumps. It follows that if $\tau_d > \frac{\ln(\max_\sigma \bar{a}_\sigma/\min_\sigma \underline{a}_\sigma)}{\min_\sigma b_\sigma}$, then W is a hybrid ISS Lyapunov function for the closed-loop system with "input" $\dot{\omega}$. The quadratic bounds and the periodic nature of the jumps imply exponential input-to-state stability of $\mathcal{A}_1$, with input $|\dot{\omega}|$. ■

4.2. Proof of Theorem 3.3

We follow similar steps to the proof of Theorem 3.1, now incorporating the jumps of the hybrid controller.

Step 1. Let $\tilde{u}_1 := u_1 - u^*(\omega)$, $\tilde{u}_2 := u_2 - u^*(\omega)$, $\tilde{u}_3 = u_3$, and $\tilde{x} := x + A_\sigma^{-1}B_\sigma(\tilde{u}_1 + u^*(\omega)) + A_\sigma^{-1}E_\sigma\omega$. The error dynamics of $\tilde{u} = (\tilde{u}_1,\tilde{u}_2,\tilde{u}_3)$ are given by $\dot{\tilde{u}}_3 = \frac{\eta}{2}$, and

$$\begin{aligned}\dot{\tilde{u}}_1 &= \frac{2\eta}{\tilde{u}_3}(\tilde{u}_2 - \tilde{u}_1) - \dot{\overbrace{u^*(\omega)}}, \\ \dot{\tilde{u}}_2 &= 2k\eta\tilde{u}_3\psi_c(\tilde{x},\tilde{u}_1,\omega) - \dot{\overbrace{u^*(\omega)}}, \qquad (30)\end{aligned}$$

where ψ_c was defined in (23). Also, we have

$$\dot{\tilde{x}} = A_\sigma\tilde{x} + \frac{2\eta}{\tilde{u}_3}A_\sigma^{-1}B_\sigma(\tilde{u}_2 - \tilde{u}_1) + A_\sigma^{-1}E_\sigma\dot{\omega}. \qquad (31)$$

We consider the Lyapunov-like function:

$$V_\sigma(\tilde{z},\omega) = \frac{(1-\theta_\sigma)}{\eta_\sigma}V_1(\tilde{u},\omega) + \frac{\theta_\sigma}{\eta_\sigma}V_2(\tilde{x},\sigma), \qquad (32)$$

where $\theta_\sigma \in (0,1)$, $\tilde{z} := (\tilde{x},\tilde{u})$, $\tilde{u} := (u_1,u_2,u_3)$, $V_1(\tilde{u},\omega) = \frac{1}{4}|\tilde{u}_2 - \tilde{u}_1|^2 + \frac{1}{4}|\tilde{u}_2|^2 + k\tilde{u}_3^2(\phi(\tilde{u}_1 + u^*(\omega),\omega) - \phi(u^*(\omega),\omega))$ and $V_2(\tilde{x},\sigma) = \tilde{x}^\mathsf{T}P_\sigma\tilde{x}$. Note that V_1 is a Lyapunov function for the accelerated hybrid gradient controller acting on *static* maps (Poveda & Li, 2021). The individual components of V_σ satisfy $\underline{\lambda}(P_\sigma)|\tilde{x}|^2 \leq V_2(\tilde{x},\sigma) \leq \bar{\lambda}(P_\sigma)|\tilde{x}|^2$ with $\bar{a}_\sigma, \underline{a}_\sigma$ as in (14); and $\frac{1+2k\ell\delta^2}{4}|\tilde{u}|^2_{\mathcal{A}_{\tilde{u}}} \leq V_1(\tilde{u},\omega) \leq \frac{1+2k\ell\Delta^2}{2}|\tilde{u}|^2_{\mathcal{A}_{\tilde{u}}}$, for all $\omega \in \Gamma$, where $\mathcal{A}_{\tilde{u}} = \{0\}\times\{0\}\times[\delta,\Delta]$, and where we used Assumptions 4 and 7. It follows that for each $\sigma \in \mathcal{S}$, V_σ satisfies $\underline{a}_\sigma|\tilde{z}|^2 \leq V_\sigma(\tilde{z}) \leq \bar{a}_\sigma|\tilde{z}|^2$, for all $\tilde{z} \in \mathbb{R}^{n+m}$ and all $\omega \in \Gamma$, where $\tilde{z} := (\tilde{x},\tilde{u})$. Next, we show that V_σ decreases during the flows of $\tilde{u}$ and $\tilde{x}$. In particular, since $\psi_c(0,\tilde{u}_1,\omega) = -\nabla_{u_1}\phi(\tilde{u}_1 + u^*(\omega),\omega)$, we have

$$\begin{aligned}\frac{1}{\eta}\nabla_{\tilde{u}_1}V_1^\top\dot{\tilde{u}}_1 &= -\frac{1}{\tilde{u}_3}|\tilde{u}_2 - \tilde{u}_1|^2 + \frac{1}{2\eta}(\tilde{u}_2 - \tilde{u}_1)^\top\dot{\overbrace{u^*(\omega)}} \\ &\quad - 2k\tilde{u}_3\psi_c(0,\tilde{u}_1,\omega)^\top(\tilde{u}_2 - \tilde{u}_1) + \frac{k}{\eta}\tilde{u}_3^2\psi_c(0,\tilde{u}_1,\omega)^\top\dot{\overbrace{u^*(\omega)}},\end{aligned}$$

and

$$\begin{aligned}\frac{1}{\eta}\nabla_{u_2}V_1^\top\dot{\tilde{u}}_2 &= \frac{1}{2\eta}(2\tilde{u} - \tilde{u}_1)^\top\dot{\tilde{u}}_2 \\ &\leq k\tilde{u}_3(2\tilde{u}_2 - \tilde{u}_1)^\mathsf{T}\psi_c(0,\tilde{u}_1,\omega) + 2\bar{a}_2|\tilde{x}||\tilde{u}_1 - \tilde{u}_2| \\ &\quad + \bar{a}_2|\tilde{x}|\,|\tilde{u}_1| - \frac{(2\tilde{u}_2 - \tilde{u}_1)^\top}{2\eta}\dot{\overbrace{u^*(\omega)}},\end{aligned}$$

where $\bar{a}_2 := k\Delta\ell_y|C||G|$. Also, using (26) and (27):

$$\begin{aligned}\frac{1}{\eta}\nabla_\omega V_1^\top\dot{\omega} &\leq -\frac{k\tilde{u}_3^2}{\eta}\left(\frac{\partial u^*}{\partial\omega}^\top\psi_c(0,\tilde{u}_1,\omega)\right)^\top\dot{\omega} \\ &\quad + \frac{k\tilde{u}_3^2}{\eta}\ell_y|H|\,|G|\,|\tilde{u}_1|\,|\dot{\omega}| \leq \frac{\bar{a}_3}{\eta}|\tilde{u}|_{\mathcal{A}_{\tilde{u}}}|\dot{\omega}|,\end{aligned}$$

with $\bar{a}_3 := k\Delta^2(\ell|\frac{\partial u^*}{\partial \omega}| + \ell_y|H||G|)$, where we used Lipschitz continuity of $\nabla_{u_1}\phi(\cdot)$. Combining the above bounds and using $\frac{1}{\eta}\nabla_{\tilde{u}_3}V_1^\top \dot{\tilde{u}}_3 = k\tilde{u}_3(\phi(\tilde{u}_1 + u^*(\omega),\omega) - \phi(u^*(\omega),\omega))$, we obtain

$$\begin{aligned}\frac{1}{\eta}\nabla V_1^\top \dot{\tilde{u}} \le & -\tilde{u}_3^{-1}|\tilde{u}_2 - \tilde{u}_1|^2 + \bar{a}_2|\tilde{x}|\,|\tilde{u}_1| + \frac{1}{\eta}\bar{a}_3|\dot{\omega}|\,|\tilde{u}|_{\mathcal{A}_{\tilde{u}}} \\ & - k\tilde{u}_3\Big(\phi(u^*(\omega),\omega) - \phi(\tilde{u}_1 + u^*(\omega),\omega) - \psi_c(0,\tilde{u}_1,\omega)^\top \tilde{u}_1\Big) \\ & + 2a_2|\tilde{x}||\tilde{u}_1 - \tilde{u}_2| + \frac{1}{2\eta}\dot{\overbrace{u^*(\omega)}}^\top \left(-\tilde{u}_2 + 2k\tilde{u}_3^2\psi_c(0,\tilde{u}_1,\omega)\right).\end{aligned} \tag{33}$$

Using strong convexity to bound the fourth term,

$$\begin{aligned}\frac{1}{\eta}\nabla V_1^\top \dot{\tilde{u}} &\le -\min\left\{\frac{1}{\Delta}, \frac{k\delta\mu}{4}\right\}|\tilde{u}|^2_{\mathcal{A}_{\tilde{u}}} + a_2|\tilde{x}||\tilde{u}|_{\mathcal{A}_{\tilde{u}}} + \frac{1}{\eta}a_3|\dot{\omega}||\tilde{u}|_{\mathcal{A}_{\tilde{u}}} \\ &\le -a_1|\tilde{u}|^2_{\mathcal{A}_{\tilde{u}}} + a_2|\tilde{x}||\tilde{u}|_{\mathcal{A}_{\tilde{u}}} - \frac{\kappa}{2}\frac{2\min\left\{\frac{1}{\Delta}, \frac{k\delta\mu}{4}\right\}}{1 + 2k\Delta^2\ell}V_1(\tilde{u},\omega)\end{aligned} \tag{34}$$

where $a_2 := 4\sqrt{2}\bar{a}_2$, $a_1 := (1-\kappa)\min\left\{\frac{1}{\Delta}, \frac{k\delta\mu}{4}\right\}$, $a_3 := \bar{a}_3 + \frac{1}{2}\max_{\omega\in\Gamma}\left|\frac{\partial u^*}{\partial\omega}\right|\sqrt{2}\max\{1, 2k\ell\Delta^2\}$, and where we used the inequalities $|\tilde{u}|^2_{\mathcal{A}_{\tilde{u}}} \le |\tilde{u}_1|^2 + 2|\tilde{u}_2 - \tilde{u}_1|^2 + 2|\tilde{u}_1|^2$ and $V_1(\tilde{u},\omega) \le \frac{1}{2}(1 + k\ell\Delta^2)|\tilde{u}|^2_{\mathcal{A}_{\tilde{u}}}$, and where the last inequality holds whenever $|\tilde{u}|_{\mathcal{A}_{\tilde{u}}} \ge \frac{2a_3}{\kappa\eta\min\left\{\frac{1}{\Delta}, \frac{k\delta\mu}{4}\right\}}|\dot{\omega}|$.

Step 2. Next, we show that the reset policy $r_0 = 1$ guarantees the decrease of V_1 during the discrete-time updates of the controller. In particular, in this case we have that $\Delta V_1 := V_1(\tilde{u}^+,\omega) - V_1(\tilde{u},\omega)$ satisfies

$$\begin{aligned}\Delta V_1 &= \frac{1}{4}|\tilde{u}_1|^2 + k\delta^2(\phi(\tilde{u}_1 + u(\omega)^*,\omega) - \phi(u^*(\omega),\omega)) - \frac{1}{4}|\tilde{u}_2|^2 \\ &\quad - \frac{1}{4}|\tilde{u}_2 - \tilde{u}_1|^2 - k\Delta^2(\phi(\tilde{u}_1 + u^*(\omega),\omega) - \phi(u^*(\omega),\omega)) \\ &\le -c_s V_1(\tilde{u},\omega),\end{aligned}$$

where $c_s := 1 - \frac{\delta^2}{\Delta^2} - \frac{1}{2\mu\Delta^2 k}$, and where we used $|\tilde{u}_1|^2 \le \frac{2}{\mu}(\phi(\tilde{u}_1 + u^*(\omega),\omega) - \phi(u^*(\omega),\omega))$ for the first inequality, and $\Delta^2 - \delta^2 \ge \frac{1}{2k\mu}$ for the second inequality. This establishes that $V_1(\tilde{u}^+,\omega) \le (1 - c_s)V_1(\tilde{u},\omega)$, with $c_s \in (0,1)$.

Step 3. We now consider the function V_2 in (32), and for each fixed σ we bound its evolution during flows and jumps triggered by the controller. In this case, we have

$$\begin{aligned}\frac{1}{\eta}\nabla V_2^\top \dot{\tilde{x}} &= \frac{1}{\eta}\tilde{x}^\mathsf{T}(A_\sigma^\mathsf{T}P_\sigma + P_\sigma A_\sigma)\tilde{x} + 2\tilde{x}^\mathsf{T}P_\sigma A_\sigma^{-1}B_\sigma\frac{(\tilde{u}_2 - \tilde{u}_1)}{\tilde{u}_3} \\ &\quad + \frac{1}{\eta}2\tilde{x}^\mathsf{T}P_\sigma A_\sigma^{-1}E_\sigma\dot{\omega} \\ &\le -\frac{1}{\eta}\underline{\lambda}(Q_\sigma)|\tilde{x}|^2 + b_2|\tilde{x}||\tilde{u}|_{\mathcal{A}_{\tilde{u}}} + 2\eta^{-1}|P_\sigma A_\sigma^{-1}E_\sigma||\tilde{x}||\dot{\omega}|,\end{aligned} \tag{35}$$

where $b_2 := 4\sqrt{2}\delta^{-1}|P_\sigma A_\sigma^{-1}B_\sigma|$. Using $V_2(\tilde{x},\sigma) \le \bar{\lambda}(P_\sigma)|\tilde{x}|^2$, we obtain

$$\frac{1}{\eta}\dot{V}_2 \le -\frac{1}{\eta}b_1|\tilde{x}|^2 + b_2|\tilde{x}||\tilde{u}|_{\tilde{\mathcal{A}}} - \frac{\kappa}{2\eta}\frac{\underline{\lambda}(Q_\sigma)}{\bar{\lambda}(P_\sigma)}V_2(\tilde{x},\sigma), \tag{36}$$

where $b_1 := (1-\kappa)\underline{\lambda}(Q_\sigma)$, which holds only if $|\tilde{x}| \ge \frac{4|P_\sigma A_\sigma^{-1}E_\sigma|}{\kappa\underline{\lambda}(Q_\sigma)}\sup_\tau|\dot{\omega}_\tau|$. Since the state of the plant and its mode do not change during discrete-time updates of the controller, we have that $V_2(\tilde{x}^+,\sigma^+) = V_2(\tilde{x},\sigma)$.

Step 4. Combining the estimates (34) and (36), we obtain that for each fixed mode σ, and outside a $|\dot{\omega}|$-neighborhood of $\{0\}\times\mathcal{A}_{\tilde{u}}$, V_σ satisfies $\dot{V}_\sigma(\tilde{z}) \le -\xi^\mathsf{T}\Lambda_\sigma\xi - b_\sigma V_\sigma(\tilde{z})$, where $\xi = (|\tilde{u}|_{\mathcal{A}_{\tilde{u}}}, |\tilde{x}|)$, b_σ is as in (21d), and Λ_σ is a 2×2 symmetric matrix with entries $\Lambda_{11} = (1-\theta)a_1$, $\Lambda_{12} = \Lambda_{12} = -\frac{1}{2}((1-\theta)\tilde{a}_2 + \theta b_2)$, and $\Lambda_{22} = \theta b_1/\eta$. It follows that when $\eta < \hat{\eta}_H$, with $\hat{\eta}_H$ given by (20), the matrix Λ_σ is positive definite. Similarly, during jumps triggered by the controller:

$$V_{\sigma^+}(\tilde{z}^+) \le \min\{1 - c_s, 1\}V_\sigma(\tilde{z}) \le V(\tilde{z}), \tag{37}$$

which implies that V_σ does not increase.

Step 6. Finally, we incorporate the switches into the error plant dynamics (23), where (σ,τ) are generated by (6). Using V_σ, we consider the extended function $W(\tilde{\vartheta}) = e^{\varrho\tau}V_\sigma(\tilde{z})$, where $\varrho > 0$ and $\tilde{\vartheta} := (\tilde{z},\sigma,\tau,\omega)$, with $\tilde{z} = (\tilde{x},\tilde{u}_1,\tilde{u}_2,\tilde{u}_3)$. We will show the existence of ϱ such that W is a hybrid ISS Lyapunov function for the HDS with error dynamics (30)–(31), exosystem (8), and switching generator (6), with respect to the compact set:

$$\mathcal{A}_3 := \left\{\tilde{\vartheta} : \tilde{x} = 0, \tilde{u}\in\mathcal{A}_{\tilde{u}},\ \sigma\in\mathcal{S},\ \tau\in[0,N_0],\ \omega\in\Gamma\right\},$$

and with "input" $\dot{\omega}$. Indeed, note that $\min_\sigma \underline{a}_\sigma|\tilde{\vartheta}|^2 \le W(\tilde{\vartheta}) \le e^{\varrho N_0}\max_\sigma \bar{a}_\sigma|\tilde{\vartheta}|^2$, where $\underline{a}_\sigma, \bar{a}_\sigma$ are as in Theorem 3.3. During flows of the system, we have that:

$$\nabla W^\top\dot{\tilde{\vartheta}} = e^{\varrho\tau}(\varrho V_\sigma(\tilde{z})\dot{\tau} + \dot{V}_\sigma(\tilde{z})) \le \left(\frac{\varrho}{\tau_d} - \min_\sigma b_\sigma\right)W(\tilde{\vartheta}),$$

which holds for all $|u|_{\mathcal{A}_{\tilde{u}}} \ge \frac{2\bar{c}_1}{\kappa\frac{1}{3}\min\{\tilde{u}_3^{-1}, \frac{\tilde{u}_3\mu}{2}\}}|\dot{\omega}|$ and $|\tilde{x}| \ge \frac{4|PA^{-1}E|}{\kappa\underline{\lambda}(Q)}|\dot{\omega}|$. Similarly, during jumps of the form $\tilde{\varrho}\in D_1$, we have that $\tilde{x}^+ = \tilde{x}$, $\tilde{u}^+ = \tilde{u}$, $\sigma^+\in\mathcal{S}$, and $\tau^+ = \tau - 1$, and thus $W(\tilde{\varphi}^+) \le e^{-\varrho + \ln(\max_\sigma\bar{a}_\sigma) - \ln(\min_\sigma\underline{a}_\sigma)}W(\tilde{\varphi})$. During jumps of the form $\tilde{\varrho}\in D_2$, we have $W(\tilde{\varphi}^+) = e^{\varrho\tau}V_\sigma(\tilde{z}^+) \le W(\tilde{\varphi})$, where we used (37). Therefore, to guarantee that W does not increase during jumps it suffices to have $\varrho > \ln(\max_\sigma\bar{a}_\sigma/\min_\sigma\underline{a}_\sigma)$ and $\varrho < \min_\sigma b_\sigma\tau_d$. Combining the upper and lower inequalities on ϱ we conclude that we need $\tau_d > \frac{\ln(\max_\sigma\bar{a}_\sigma/\min_\sigma\underline{a}_\sigma)}{\min_\sigma b_\sigma}$, which establishes the result. ■

4.3. Proof of Theorem 3.2

We follow similar steps as in the proof of Theorem 3.3. Since ω is now constant, we have that $\dot{\omega} = 0$, and since we focus on a single mode of the plant we drop the subscript σ. The error dynamics (30) become $\dot{\tilde{u}}_3 = \frac{\eta}{2}$ and

$$\dot{\tilde{u}}_1 = \frac{2\eta}{\tilde{u}_3}(\tilde{u}_2 - \tilde{u}_1),\ \ \dot{\tilde{u}}_2 = 2k\eta\tilde{u}_3\psi_c(\tilde{x},\tilde{u}_1,\omega), \tag{38}$$

while the dynamics of $\tilde{x}$ are still given by (31). By construction, and under Assumption 6, the function V defined in (32) is radially unbounded and positive definite with respect to the compact set $\{0\}\times\mathcal{A}_{\tilde{u}}$. Along the dynamics (38), the function V_1 still satisfies (33). Using convexity and the Lipschitz property of $\nabla_u\phi$, we obtain:

$$\begin{aligned}\frac{1}{\eta}\nabla V_1^\top\dot{\tilde{u}} \le & -2\Delta^{-1}|\tilde{u}_2 - \tilde{u}_1|^2 + a_2|\tilde{x}||\tilde{u}_1| + 2a_2|\tilde{x}||\tilde{u}_1 - \tilde{u}_2| \\ & - a_4|\nabla\phi(\tilde{u}_1 + u^*)|^2,\end{aligned}$$

where $a_4 := \frac{\delta k}{2\ell}$. Similarly, from (35), we now have that

$$\frac{1}{\eta}\nabla V_2^\top\dot{\tilde{x}} \le -\frac{1}{\eta}\underline{\lambda}(Q)|\tilde{x}|^2 + b_2|\tilde{x}||\tilde{u}|_{\mathcal{A}_{\tilde{u}}}. \tag{39}$$

where $b_2 := 2\delta^{-1}|PA^{-1}B|$. It follows that V satisfies

$$\begin{aligned}\nabla V^\top\dot{\tilde{u}} \le & -\xi^\mathsf{T}\Lambda\xi - a_4(1-\theta)|\nabla\phi(\tilde{u}_1 + u^*)|^2 \\ & - \kappa\theta\frac{\underline{\lambda}(Q)}{\eta}|\tilde{x}|^2 + (1-\theta)a_2|\tilde{x}||\tilde{u}_1|,\end{aligned} \tag{40}$$

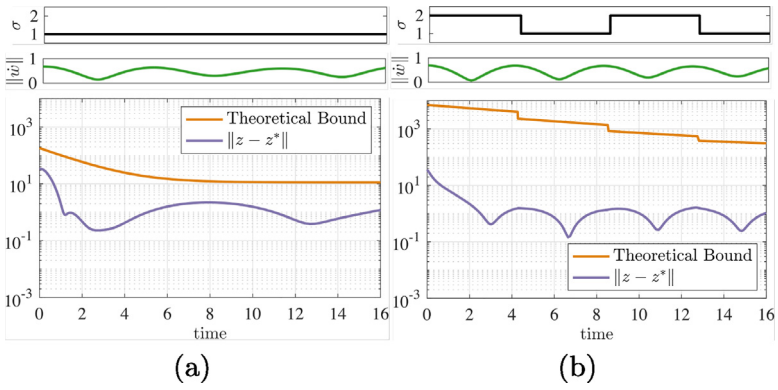

Fig. 2. Tracking error of gradient flow controller (10). (a) No plant switching. (b) Plant switches between two modes.

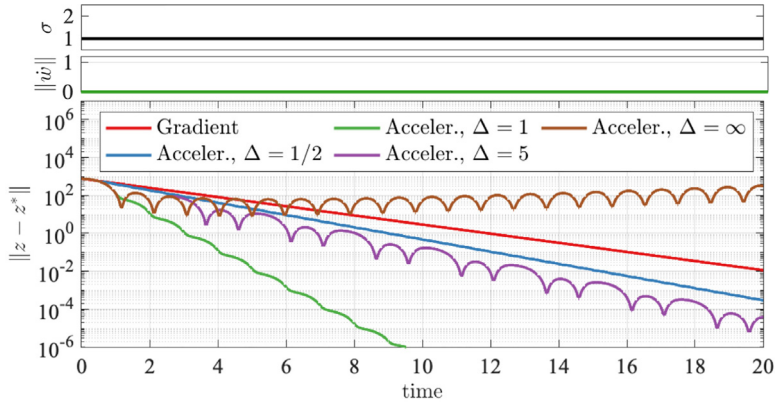

Fig. 3. Comparison Gradient Flow vs Accelerated Gradient.

with $\xi = (|\tilde{u}_2 - \tilde{u}_1|, |\tilde{x}|)$, and where $\Lambda \in \mathbb{R}^{2\times 2}$ is a symmetric matrix with entries given by $\Lambda_{11} = (1-\theta)\Delta^{-1}$, $\Lambda_{12} = \Lambda_{21} = -\frac{1}{2}((1-\theta)2a_2 + \theta b_2)$, and $\Lambda_{22} = -\theta(1-\kappa)\underline{\lambda}(Q)/2$. We now consider two possible scenarios:

Case 1: Suppose that $-\kappa\theta\frac{\underline{\lambda}(Q)}{\eta}|\tilde{x}|^2 + (1-\theta)a_2|\tilde{x}||\tilde{u}_1| \leq 0$. In this case, we have $\dot{V} \leq -\xi^\top\Lambda\xi - (1-\theta)a_4|\nabla\phi(\tilde{u}_1+u^*)|^2$; since $\Lambda \succ 0$, and using the convexity of ϕ, we conclude that $\dot{V} < 0$ for all $\eta \in (0, \bar{\eta}_s)$ and $\tilde{z} \neq (0, u^*)$.

Case 2: Suppose $-\kappa\theta\frac{\underline{\lambda}(Q)}{\eta}|\tilde{x}|^2 + (1-\theta)a_3|\tilde{x}||\tilde{u}_1| > 0$. In this case, we note that $\eta \in (0, \bar{\eta}_s)$ implies $\sqrt{\frac{1-\theta}{\theta}\frac{4\ell a_3^2\eta}{\kappa^2 b_1\delta k}} \leq \ell_0$ and, by combining this observation with Assumption 6 we conclude that $|\nabla\phi(\tilde{u}_1+u^*)| \geq \sqrt{\frac{1-\theta}{\theta}\frac{4\ell a_3^2\eta}{\kappa^2 b_1\delta k}}|\tilde{u}_1|$ and thus $\dot{V} \leq -\xi^\top\Lambda\xi - \kappa\theta\frac{\underline{\lambda}(Q)}{\eta}|\tilde{x}|^2 - (1-\kappa)(1-\theta)\frac{k\delta}{4\ell}|\nabla\phi(\tilde{u}_1+u^*)|^2$. Since $\Lambda \succ 0$ when $\eta \in (0, \bar{\eta}_s)$, we have that $\dot{V} < 0$ outside a neighborhood of $\{0\}\times\mathcal{A}_{\tilde{u}}$. Finally, we show that if $\Delta > \delta$, the Lyapunov function V does not increase during jumps of controller. Indeed, the reset policy $r_0 = 0$ implies that $V(\tilde{z}^+) - V(\tilde{z}) = \frac{k}{4}(\delta^2 - \Delta^2)\big(\phi(\tilde{u}_1+u^*) - \phi(u^*)\big) \leq 0$, where the inequality holds because $\delta < \Delta$. The strong decrease of V during flows outside of a neighborhood of $\{0\}\times\mathcal{A}_{\tilde{u}}$, the non-increase during jumps, and the periodic hybrid time domain of the solutions guarantee uniform convergence of $(\tilde{x}, u_1, u_2)$ from compact sets to a neighborhood of $(0, u^*, u^*)$ via (Goebel et al., 2012, Ch.8), which establishes item (a) of Theorem 3.2. Item (b) follows by the fact that $\dot{V} \leq 0$ outside a neighborhood of $\{0\}\times\mathcal{A}_{\tilde{u}}$, which implies that in this set $V(t,j) \leq V(\underline{t}_j, j)$ for each (t,j) in the domain of the solution, and the fact that by construction of (32) we have $ku_3(t,j)^2(\phi(u_1(t,j)) - \phi^*) \leq V(t,j)$, which leads to the bound of the theorem with $c_j := k^{-1}V(\underline{t}_j, j)$. ■

5. Numerical examples

To illustrate our results, we consider a plant with two modes $\mathcal{S} = \{1,2\}$, $n = 10$ states, $m = 5$ inputs, $p = 5$ outputs, and $q = 6$ exogenous disturbances. We consider cost functions $\phi_u(u) = u^\top Ru$, $\phi_y(y) = (y - y_{\text{ref}})^\top Q(y - y_{\text{ref}})$ where $R \in \mathbb{R}^{m\times m}$, $R \succ 0$, $Q^{p\times p}$, $Q \succ 0$, and $y_{\text{ref}} \in \mathbb{R}^p$ is a constant reference signal. We first consider the gradient flow controller (10), which generates the trajectories shown in Fig. 2. In particular, Fig. 2-(a) shows the bound established in Theorem 3.1, when the plant has a single mode (i.e., $\sigma = 1$). On the other hand, Fig. 2-(b) shows the bound corresponding to the case when the switching signal is time-varying. Next, we consider the hybrid accelerated gradient controller of Section 3.2. When the disturbance ω_t is constant and the plant has a single operating mode (i.e., $\sigma = 1$), Fig. 3 compares the performance of the hybrid controller versus the gradient-flow controller. Different reset parameters are considered, with $\Delta = 0.5, 1, 5$; we also consider $\Delta = \infty$, corresponding to (4). In the latter case, the simulation shows that the trajectories diverge. Similarly, Fig. 4-(a) shows the bound of Theorem 3.3, when ω_t is time-varying and the switching signal σ is constant at all times. Fig. 4-(b) considers the case when the switching signal is time-varying. We note that in this simulation the time horizon has been rescaled in order to illustrate the behavior of the controller under switching of the plant. Finally, Fig. 5 illustrates the bound in Theorem 3.2. In this case, we consider a scalar plant ($n = m = p = 1$) with a single mode ($|\mathcal{S}| = 1$) and cost function $\phi_t(u) = 0.25(Gu + H\omega_t - y_{\text{ref}})^4$, where $y_{\text{ref}} \in \mathbb{R}$. Note that ϕ_t satisfies Assumptions 4 and 6 on compact sets. Two important observations follow from Fig. 5. First, the simulations

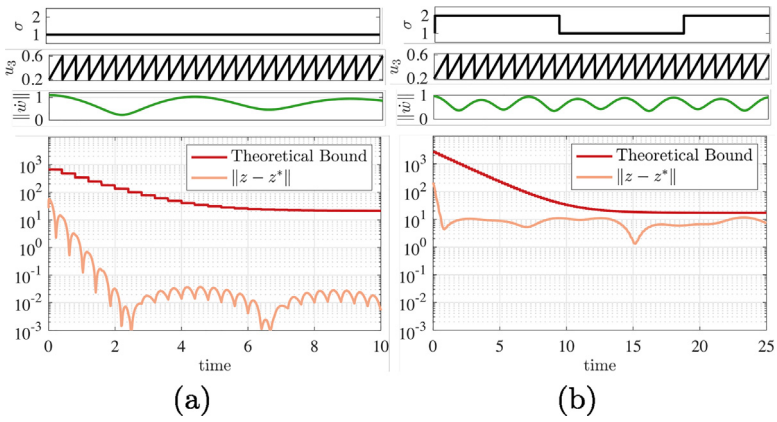

Fig. 4. Tracking error of accelerated gradient controller. (a) No plant switching. (b) Switched plant.

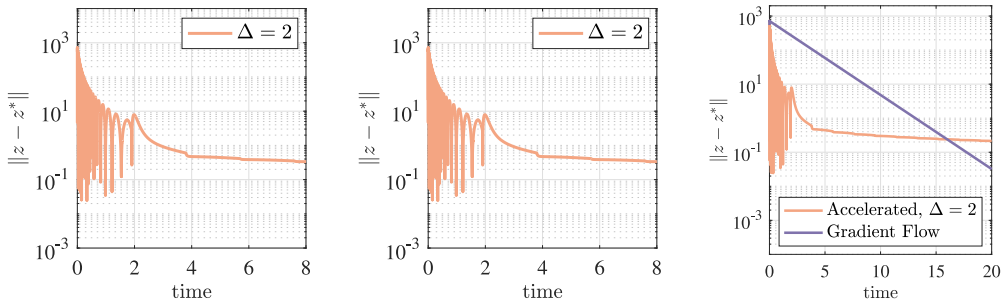

Fig. 5. Tracking error of accelerated gradient controller with polynomial cost function and different values of Δ.

suggest that in this case smaller restarting times Δ can improve transient performance. Second, the simulation illustrates that the control signal converges only to a neighborhood of the optimal point, thus validating the conclusion of Theorem 3.2. The neighborhood of convergence can be characterized by observing that Assumption 6 implies $(u - u_{\text{ref}})^2 > \nu_0^2$, and thus $\nu_0^2 = \ell_0$. Finally, the right plot in Fig. 5 compares the regulation error of the gradient flow controller versus the hybrid accelerated gradient controller. The figure shows that the accelerated gradient controller achieves faster convergence compared to the gradient descent-based controller, but the convergence is guaranteed only up to a neighborhood of z_t^*.

6. Conclusions

We addressed the problem of online optimization of switched linear time invariant dynamical systems via optimization-based controllers. We introduced two feedback controllers, one based on gradient descent flows, and a one based on a hybrid regularization of accelerated gradient systems with dynamic momentum. Under a suitable average dwell-time constraint on the switching signal, we established ISS properties for the closed-loop system with input being the time-derivative of the disturbance. This result generalizes previous works on time-invariant optimization problems and non-switching plants. Future research directions will focus on developing tighter interconnection bounds between hybrid plants and hybrid controllers via small gain arguments.

Acknowledgments

Supported by NSF CMMI 2044946, NSF CAREER 2144076, AFOSR YIP FA9550-22-1-0211.

References

Absil, P.-A., & Kurdyka, K. (2006). On the stable equilibrium points of gradient systems. *Systems & Control Letters*, *55*(7), 573–577.

Bianchin, G., Cortés, J., Poveda, J. I., & Dall'Anese, E. (2021). Time-varying optimization of LTI systems via projected primal-dual gradient flows. *IEEE Transactions on Control of Network Systems*, *9*(1), 474–486.

Bianchin, G., & Pasqualetti, F. (2020). Gramian-based optimization for the analysis and control of traffic networks. *IEEE Transactions on Intelligent Transportation Systems*, *21*(7), 3013–3024.

Brunner, F. D., Dürr, H.-B., & Ebenbauer, C. (2012). Feedback design for multi-agent systems: A saddle point approach. In *IEEE conf. on decision and control* (pp. 3783–3789).

Colombino, M., Dall'Anese, E., & Bernstein, A. (2020). Online optimization as a feedback controller: Stability and tracking. *IEEE Transactions on Control of Network Systems*, *7*(1), 422–432.

Gaudio, J. E., Annaswamy, A. M., Bolender, M. A., & Lavretsky, E. (2021). A class of high order tuners for adaptive systems. *IEEE Control Systems Letters*, *5*(2), 391–396.

Gazi, V. (2007). Output regulation of a class of linear systems with switched exosystems. *International Journal of Control*, *80*(10), 1665–1675.

Goebel, R., Sanfelice, R. G., & Teel, A. R. (2012). *Hybrid dynamical systems: modeling stability, and robustness*. Princeton, NJ: Princeton University Press.

Hauswirth, A., Bolognani, S., Hug, G., & Dörfler, F. (2020). Timescale separation in autonomous optimization. *IEEE Transactions on Automatic Control*, *66*(2), 611–624.

Hespanha, J. P., & Morse, A. S. (1999). Stability of switched systems with average dwell-time. In *IEEE conf. on decision and control, Phoenix, AZ, USA* (pp. 2655–2660).

Jokic, A., Lazar, M., & Bosch, P. P. V. D. (2009). On constrained steady-state regulation: Dynamic KKT controllers. *IEEE Transactions on Automatic Control*, *54*(9), 2250–2254.

Khalil, H. K. (2002). *Nonlinear systems* (2nd ed.). Upper Saddle River, NJ: Prentice Hall.

Lawrence, L. S. P., Nelson, Z. E., Mallada, E., & Simpson-Porco, J. W. (2018). Optimal steady-state control for linear time-invariant systems. In *IEEE conf. on decision and control, Miami Beach, FL, USA* (pp. 3251–3257).

Lawrence, L. S., Simpson-Porco, J. W., & Mallada, E. (2020). Linear-convex optimal steady-state control. *IEEE Transactions on Automatic Control*, *66*(11), 5377–5384.

Marconi, L., & Teel, A. R. (2010). A note about hybrid linear regulation. In *IEEE conf. on decision and control* (pp. 1540–1545).

Menta, S., Hauswirth, A., Bolognani, S., Hug, G., & Dörfler, F. (2018). Stability of dynamic feedback optimization with applications to power systems. In *Annual conf. on communication, control, and computing* (pp. 136–143).
O'Donoghue, B., & Candes, E. (2015). Adaptive restart for accelerated gradient schemes. *Foundations of Computational Mathematics*, *15*(3), 715–732.
Poveda, J. I., & Li, N. (2019). Inducing uniform asymptotic stability in non-autonomous accelerated optimization dynamics via hybrid regularization. In *IEEE conf. on decision and control, Nice, France* (pp. 3000–3005).
Poveda, J. I., & Li, N. (2021). Robust hybrid zero-order optimization algorithms with acceleration via averaging in time. *Automatica*, *123*, Article 109361.
Poveda, J. I., & Teel, A. R. (2020). The heavy-ball ODE with time-varying damping: Persistence of excitation and uniform asymptotic stability. In *American control conference* (pp. 773–778).
Prieur, C., Queinnec, I., Tarbouriech, S., & Zaccarian, L. (2018). Analysis and synthesis of reset control systems. *Foundations and Trends in Systems and Control*, *6*, 117–338.
Shi, B., Du, S. S., Jordan, M. I., & Su, W. J. (2021). Understanding the acceleration phenomenon via high-resolution differential equations. *Mathematical Programming*.
Su, W., Boyd, S., & Candes, E. (2014). A differential equation for modeling nesterov's accelerated gradient method: Theory and insights. In *Advances in neural information processing systems, Vol. 27* (pp. 2510–2518). Curran Associates.
Teel, A. R., Moreau, L., & Nesic, D. (2003). A unified framework for input-to-state stability in systems with two time scales. *IEEE Transactions on Automatic Control*, 1526–1544.
Wibisono, A., Wilson, A. C., & Jordan, M. I. (2016). A variational perspective on accelerated methods in optimization. *Proceedings of the National Academy of Sciences*, *113*(47), E7351–E7358.
Zhang, J., Uribe, C. A., Mokhtari, A., & Jadbabaie, A. (2018). Achieving acceleration in distributed optimization via direct discretization of the heavy-ball ODE. arXiv:1811.02521.
Zheng, T., Simpson-Porco, J. W., & Mallada, E. (2020). Implicit trajectory planning for feedback linearizable systems: A time-varying optimization approach. In *American control conference* (pp. 4677–4682).

Gianluca Bianchin is an Assistant Professor in the ICTEAM Institute at the *Université Catholique de Louvain.* He was a Postdoctoral Scholar in the ECEE Department at the University of Colorado Boulder from 2020 to 2022. He received the Doctor of Philosophy degree in Mechanical Engineering at the University of California Riverside in 2020, the Laurea degree in Information Engineering, and the Laurea Magistrale degree (Summa Cum Laude) in Controls Engineering from the University of Padova, Italy, in 2012 and 2014, respectively. In 2018 he joined the Pacific Northwest National Laboratory as a Graduate Intern and in 2019 the Bosch Research Center as a Research Intern. His main research interests are in the modeling, analysis, and control of large-scale networked systems, with an application focus on transportation networks. He was the recipient of the Dissertation Year Award and of the Dean's Distinguished Fellowship Award from the University of California Riverside.

Jorge I. Poveda received the M.Sc. and Ph.D. degrees in Electrical and Computer Engineering from the University of California at Santa Barbara, USA, in 2016 and 2018, respectively. After that, he was a Postdoctoral Fellow with Harvard University, Cambridge, MA, USA, before joining the Electrical, Computer, and Energy Engineering department at the University of Colorado, Boulder, from 2019 until 2022. He is currently an Assistant Professor in the Electrical and Computer Engineering department at the University of California, San Diego.

Prof. Poveda was the recipient of the CRII and CAREER Awards from the National Science Foundation, the Young Investigator Award from the Air Force Office of Scientific Research, the campus-wide Research and Innovation Faculty Fellowship at the University of Colorado, and the CCDC Outstanding Scholar Fellowship and Best Ph.D. Dissertation awards at UC Santa Barbara. He has also co-authored papers nominated for the Best Student Paper Awards at the IEEE Conference on Decision and Control in 2017 and 2021. His areas of interest include nonlinear and hybrid control, model-free optimization, and distributed control.

Emiliano Dall'Anese is an Assistant Professor in the Department of Electrical, Computer, and Energy Engineering at the University of Colorado Boulder, and an affiliate Faculty with the Department of Applied Mathematics. He received the Ph.D. in Information Engineering from the Department of Information Engineering, University of Padova, Italy, in 2011. From January 2011 to November 2014, he was a Postdoctoral Associate at the Department of Electrical and Computer Engineering of the University of Minnesota, and from December 2014 to July 2018 he was a Senior Researcher at the National Renewable Energy Laboratory. %His research interests span the areas of optimization, control, and learning, with current applications in power systems, transportation networks, and healthcare.

He received the National Science Foundation CAREER Award in 2020, and the IEEE PES Prize Paper Award in 2021.